Designing and exploring active N′-[(5-nitrofuran-2-yl) methylene] substituted hydrazides against three Trypanosoma cruzi strains more prevalent in Chagas disease patients

ARTICLE *in* EUROPEAN JOURNAL OF MEDICINAL CHEMISTRY · APRIL 2015

Impact Factor: 3.45 · DOI: 10.1016/j.ejmech.2015.03.066

European Journal of Medicinal Chemistry 96 (2015) 330–339

Contents lists available at ScienceDirect

European Journal of Medicinal Chemistry

journal homepage: http://www.elsevier.com/locate/ejmech

Original article

Designing and exploring active *N*′-[(5-nitrofuran-2-yl) methylene] substituted hydrazides against three *Trypanosoma cruzi* strains more prevalent in Chagas disease patients

Fanny Palace-Berl [a, *], Kerly Fernanda Mesquita Pasqualoto [b], Salomão Dória Jorge [d], Bianca Zingales [c], Rodrigo Rocha Zorzi [a], Marcelo Nunes Silva [c], Adilson Kleber Ferreira [d], Ricardo Alexandre de Azevedo [d], Sarah Fernandes Teixeira [d, e], Leoberto Costa Tavares [a]

[a] Department of Biochemical and Pharmaceutical Technology, Faculty of Pharmaceutical Sciences, University of São Paulo, SP, Brazil
[b] Biochemistry and Biophysics Laboratory, Butantan Institute, SP, Brazil
[c] Department of Biochemistry, Chemistry Institute, University of São Paulo, SP, Brazil
[d] Department of Immunology, Biomedical Sciences Institute, University of São Paulo, SP, Brazil
[e] Cell and Molecular Therapy Center – NUCEL/NETCEM, School of Medicine, University of São Paulo, São Paulo, SP, Brazil

ARTICLE INFO

Article history:
Received 27 October 2014
Received in revised form
26 February 2015
Accepted 30 March 2015
Available online 1 April 2015

Keywords:
N′-[(5-nitrofuran-2-yl) methylene] substituted hydrazides
Chagas disease
Trypanosoma cruzi strains
Exploratory data analysis

ABSTRACT

Chagas disease affects around 8 million people worldwide and its treatment depends on only two nitroheterocyclic drugs, benznidazole (BZD) and nifurtimox (NFX). Both drugs have limited curative power in chronic phase of disease. Nifuroxazide (NF), a nitroheterocyclic drug, was used as lead to design a set of twenty one compounds in order to improve the anti-*Trypanosoma cruzi* activity. Lipinski's rules were considered in order to support drug-likeness designing. The set of *N*′-[(5-nitrofuran-2-yl) methylene] substituted hydrazides was assayed against three *T. cruzi* strains, which represent the discrete typing units more prevalent in human patients: Y (TcII), Silvio X10 cl1 (TcI), and Bug 2149 cl10 (TcV). All the derivatives, except one, showed enhanced trypanocidal activity against the three strains as compared to BZD. In the Y strain 62% of the compounds were more active than NFX. The most active compound was *N*′-((5-nitrofuran-2-yl) methylene)biphenyl-4-carbohydrazide (C20), which showed IC_{50} values of 1.17 ± 0.12 μM; 3.17 ± 0.32 μM; and 1.81 ± 0.18 μM for Y, Silvio X10 cl1, and Bug 2149 cl10 strains, respectively. Cytotoxicity assays with human fibroblast cells have demonstrated high selectivity indices for several compounds. Exploratory data analysis indicated that primarily topological, steric/geometric, and electronic properties have contributed to the discrimination of the set of investigated compounds. The findings can be helpful to drive the designing, and subsequently, the synthesis of additional promising drugs against Chagas disease.

1. Introduction

Chagas disease (CD) is caused by the protozoan *Trypanosoma cruzi*, which can be transmitted by two predominant modes: vectorial, through infected feces/urine of triatomine bugs ('kissing bugs'), and by blood transfusion. Congenital transmission and oral infection by the ingestion of parasites in contaminated food, are also considered as important [1].

CD currently affects an estimated 8 million people in 21 countries in Latin America and is spreading by human migration to several countries in Europe, Canada, USA, Japan and Australia. It is considered the parasitic disease with the greatest socioeconomic impact in Latin America, being responsible for lost productivity costing US$ 1.2 billion annually [2].

CD is among the most neglected diseases. Since the 1970s, the treatment for Chagas disease is dependent on only two drugs, benznidazole (BZD, *N*′-benzyl-2-(2-nitroimidazolyl)acetamide) and nifurtimox (NFX, 3-methyl-4-(5-nitrofurfurylidene-amino)tetrahydro-4H-1,4-thiazine-1,1-dioxide) (Fig. 1A). Both nitroheterocyclic drugs require a prolonged treatment, cause severe side effects and have limited curative power in the chronic phase [1].

* Corresponding author. Av. Prof. Lineu Prestes, 580, São Paulo, SP 05508-000, Brazil.
E-mail address: palaceberlf@usp.br (F. Palace-Berl).

http://dx.doi.org/10.1016/j.ejmech.2015.03.066
0223-5234/

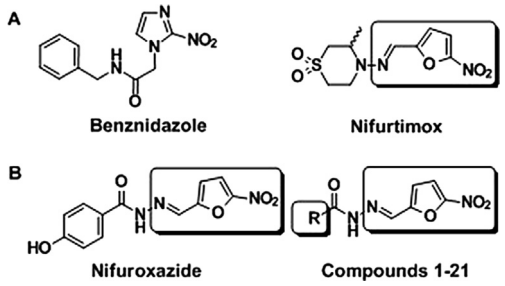

Fig. 1. (A) Chemical structure of benznidazole and nifurtimox. (B) Chemical structure of nifuroxazide, the lead compound, and scaffold of the designed compounds (c1–c21). Similar portions of nifuroxazide and nifurtimox structures were maintained in the designed compounds. The region where molecular modifications (R) were carried out is pointed out.

The reasons for treatment failures are unknown. NFX and BZD have shown different efficacies according to disease endemic areas [3]. In addition, experimental evidence in murine models indicates that both drugs exhibit a broad range of divergent activities against different *T. cruzi* strains, and natural resistance to NFX and BZD has been reported [4,5].

The biological and genetic diversity of *T. cruzi* strains have long been recognized. The strains are divided into six discrete typing units (DTUs) named as TcI to TcVI [6]. The ecological and epidemiological characteristics of *T. cruzi* DTUs have been recently reviewed [7–9]. DTUs TcI, TcII, TcV and TcVI are agents of human disease with dissimilar prevalence in different regions of Latin America. TcI is a major agent of human infection in Mexico, Central America, Amazonia and northern countries of South America. TcII predominates in patients in Brazil, whereas TcV and TcVI prevail in patients in the other countries of the Southern Cone region of South America. No apparent DTU association with natural resistance to BZD and NFX has been observed so far [10,11].

Given the unsatisfactory performance of the currently available drugs, new approaches on more specific chemotherapy for CD have been advanced in the last three decades and novel potential drug targets have already been described [2]. Ergosterol biosynthesis inhibitors, such as posaconazole and ravuconazole (E1224, prodrug), showed promising preliminary results [12]. Phase IIa clinical trials for evaluation of antiparasitic activity of both drugs in chronic patients have recently been concluded, but with unsatisfactory results [13,14]. An approach regarding the CD drug discovery and development scenery in 2013/2014 can be found elsewhere [15].

Previous data from our group have shown that some nifuroxazide (NF), 4-hydroxy-*N*′-(5-nitro-2-furfuryliden) benzohydrazide derivatives (Fig. 1B), show trypanocidal activity against epimastigote forms of the Y (DTU TcII) strain [16–18]. In addition, we have also reported that benzofuroxan derivatives and 5-nitro-2-furfuriliden derivatives are active against multidrug-resistant *Staphylococcus aureus* strains [16–20]. Although the NF mode of action is not fully elucidated, previous studies have suggested that NF antimicrobial activity would be related to the nitro group reduction and formation of free radical toxic species [16–18]. Being *T. cruzi* partially deficient in free radical detoxification mechanisms, these intermediates could affect its metabolism. The trypanocidal activity of NFX involves the generation of nitro anion radical by nitroreductases which, in the presence of oxygen, form reactive intermediates deleterious to the parasite [19,21–23]. Nifurtimox and eflornithine combination therapy have been considered the first-line treatment in second-stage gambiense human African trypanosomiasis (HAT) [24]. This fact would support the interest to investigate the trypanocidal action of new nitroderivative compounds.

NF analogs were synthesized (Fig. 1B), herein, in order to identify more active compounds against strains representing the DTUs more prevalent in human patients: TcI, TcII, and TcV [15]. Molecular modifications on the phenol group of NF scaffold were carried out in order to obtain physicochemical diversity. 'Lipinski's Rule of 5' was considered to support the design of drug-likeness [25–28]. The (5-nitrofuran-2-yl)methanamine moiety remained unchanged in order to preserve the similarity with the pharmacophoric group of NF and NFX. The energetically favorable conformation of each compound was selected by applying molecular modeling methods. Then, molecular properties of distinct nature (electronic, steric, hydrophobic, topological and geometric) were calculated to perform exploratory data analysis, which comprises hierarchical cluster analysis (HCA) and principal component analysis (PCA) [29,30]. The compounds were discriminated based on either similarity indices (HCA) or linear combination (PCA) in order to establish some qualitative structure–activity relationships.

2. Results and discussion

2.1. Chemistry

The set of 5-nitro-2-furfuriliden derivatives was obtained as shown in Scheme 1A. Molecular modifications were based on the influence of physicochemical properties, mainly hydrophobicity, represented by the calculated *n*-octanol/water partition coefficient (ClogP) [27,28] and steric/hydrophobic properties, represented by molar refractivity (MR) [31] in order to achieve structure diversity with the inclusion of aryl, alkyl and cicloalkyl substituent groups (Fig. 1). Recently, ClogP was pointed out as an important descriptor for anti-*T. cruzi* activity, showing high correlation with IC_{50} values against epimastigote forms of *T. cruzi* (Y strain) [18]. Furthermore, the designed compounds presented high degree of drug-likeness, regarding 'Lipinski's Rule of 5' [25,26] (see Scheme 1B).

The hydrazides were obtained from carboxylic acids through consecutive esterification and hydrazinolysis reactions, without isolating the corresponding methyl esters [32]. The hydrazinolysis reactions provided yields from 67 to 97%. 5-nitro-2-furfuriliden derivatives (c1–c21) were obtained by nucleophilic addition of hydrazides with 5-nitro-2-furaldehyde, and the yield ranged from 65 to 98%, as previously reported [18,33]. Regarding the nucleophilic addition step, compounds with low ClogP, i.e. high solubility in water, such as compounds c1 [$-CH_3$], c2 [$-C_5H_{11}$], c3 [$-C_5H_9$], c4 [$-O(tert\text{-}C_4H_9)$], c6 [$-C_6H_{11}$], and c11 [$-C_8H_{17}$], were synthesized using ethanol as reaction medium. Among the advantages of this method are: the isolation process, the reduction of impurities, and the improvement of yield. However, this approach requires more reaction time, and can be used only for hydrophilic compounds [34].

The structural elucidation of compounds c1–c21 was confirmed through ^1H and ^{13}C NMR spectra analysis, considering chemical shifts (δ) related to the residual solvent peak or internal standard (see Supplementary Material). Compounds showed characteristic NMR spectra, and compound c19 [$-C_6H_4$-4-OC_4H_9] was chosen to illustrate the analysis (Fig. 2). Regarding ^1H NMR spectrum of compound c19 (Fig. 2A), singlet signals can be observed around δ 12 ppm and δ 8 ppm, indicating the protons of *N*-acylhydrazones group (see Fig. 2: H_8 and H_6, respectively). The ^{13}C NMR spectrum of compound c19 has two characteristic peaks, as illustrated in Fig. 2B, one around δ 170 ppm, related to C_9 (carboxyl carbon), and other near 130 ppm, which is characteristic of C_6 (azomethine carbon).

2.2. Anti-T. cruzi activity assays

The biological activity of compounds c5, c9, c10 and c15 against

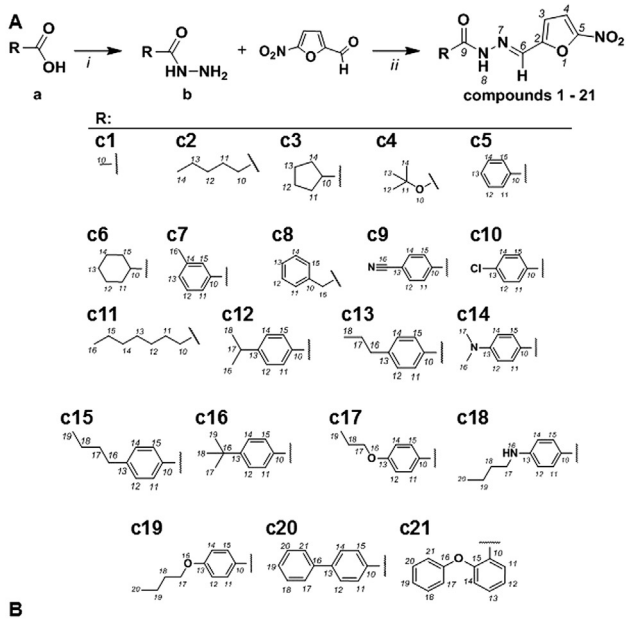

B

Compounds	c1	c2	c3	c4	c5	c6	c7	c8	c9	c10	c11
$ClogP_{G\text{-}SLN}$	-0.97	2.23	1.87	0.58	0.70	1.16	1.18	0.73	0.57	1.36	3.57
MW (g)	197.15	222.28	251.24	255.23	259.22	265.27	273.24	273.24	284.23	293.66	295.33
H- Donor	1	1	1	1	1	1	1	1	1	1	1
H- Acceptor	7	7	7	7	7	7	7	7	8	7	7
MR	46.53	64.96	63.14	60.24	67.2	67.74	72.25	71.26	72.93	72.01	78.77
n° atoms	21	33	31	30	28	34	31	31	29	28	42
R- Bonds	5	7	4	5	4	5	4	5	4	4	10
PSA (Å^2)	100.42	100.42	100.42	100.42	100.42	100.42	100.42	100.42	124.21	100.42	100.42

Compounds	c12	c13	c14	c15	c16	c17	c18	c19	c20	c21
$ClogP_{G\text{-}SLN}$	1.89	3.46	0.86	2.55	2.10	1.55	2.85	2.01	3.70	2.26
MW (g)	301.11	301.30	302.29	315.32	315.32	317.30	330.34	331.32	335.31	351.09
H- Donor	1	1	1	1	1	1	2	1	1	1
H- Acceptor	7	7	8	7	7	8	8	8	7	8
MR	81.4	81.45	81.63	86.05	85.87	82.94	91.27	87.54	92.34	93.45
n° atoms	37	22	36	40	40	38	42	41	38	39
R- Bonds	5	6	5	7	5	7	8	8	5	6
PSA (Å^2)	100.42	100.42	103.66	100.42	100.42	109.65	112.45	109.65	100.42	109.65

Lipinski' 'Rule of 5': logP < 5, MW < 500, H- Donor <5, H- Acceptor < 10; Ghose, Viswanadhan, Wendoloski, 1999: logP -0.4 to 5.6, MR 40 to 130, MW 180 to 500, n° of atoms 20 to 70, PSA < 140 Å^2; Veber *et. all*, 2002: R- Bonds < 10, PSA < 140 Å^2.

Scheme 1. Synthetic route of 5-nitro-2-furfuriliden derivatives and molecular properties considered to design compounds c1–c21. (A) Reaction conditions: (*i*) CH_3OH, H_2SO_4/reflux/4 h; N_2H_4 80% in H_2O/75 °C/30 min; (*ii*) 5-Nitro-2-furaldehyde, H_2O, H_2SO_4, CH_3COOH, C_2H_5OH/reflux/1 h or C_2H_5OH/r.t./6–8 h (for compounds presenting high water solubility). NMR spectra attributions were carried out in accordance with the numbered chemical structure. Compounds numbered in ascending order of molar weight. (B) Properties of compounds c1–c21: calculated partition coefficient by Ghose-SLN method ($ClogP_{G\text{-}SLN}$) [39]; MW: molecular weight (u or g); H- Donor: H-bond donors (expressed as the sum of OH and NH); H- Acceptor: H-bond acceptors (expressed as the sum of N and O); MR: molar refractivity; n° atoms: number of atoms in the molecule; R- Bonds: rotatable bonds; PSA: polar surface area (Å^2) [62].

epimastigotes forms of the Y strain had been previously determined [17]. The anti-*T. cruzi* activity of the designed compounds was determined, herein, in epimastigote forms of three *T. cruzi* strains. The selected strains belong to DTUs with high prevalence in patients in different Latin American regions: Silvio X10 cl1 (TcI), Y (TcII), and Bug 2149 cl10 (TcV) [6,9]. Parasites in exponential growth phase were incubated with different concentrations of the compounds (c1–c21) for 72 h at 28 °C. NFX, BZD, and the lead compound, NF, were incubated in parallel and used as controls. In order to solubilize the compounds and control drugs, DMSO was added to the medium, not exceeding 1.0% of the final concentration [35,36]. The anti-*T. cruzi* activity was expressed as IC_{50} values, which represent the compound concentration capable of inhibiting 50% of parasite growth (Table 1) (see also Supplementary Material). Then, the IC_{50} values were transformed into potency ($log1/IC_{50}$ or pIC_{50}) (Table 1). The compounds displaying higher values of pIC_{50} present better inhibitory activity.

Data in Table 1 show that the 5-nitro-2-furfuriliden derivatives presented IC_{50} values (μM) around 3–250-fold lower than the lead compound NF, regarding the Y and Bug 2149 cl10 strains. This indicates that the molecular modifications were efficacious. Considering the anti-*T. cruzi* activity of BZD, all investigates derivatives, except compound c14, showed improved trypanocidal activity against the three strains. In the Y strain 13 out of 21 compounds (62%) were more active than NFX. However, the efficacy of the designed compounds against Silvio and Bug strains was lower (4 out of 21 compounds). In fact, only 4 derivatives (15%) were more active than NFX (Table 1). Interestingly, the Silvio and Bug strains were approximately two-fold more susceptible to NFX than the Y strain (Table 1). This data set has shown the variation of drug sensitivity among *T. cruzi* strains.

Compound c20 [$-C_6H_4$-4-C_6H_5] was the most active against Y, Silvio X10 cl1 and Bug 2149 cl10 strains (IC_{50} values from 1.17 to 3.17 μ*M*), followed by compounds c15 [$-C_6H_4$-4-C_4H_9], c18 [$-C_6H_4$-4-NC_4H_9] and c19 [$-C_6H_4$-4-OC_4H_9]. Conversely, compound c14 [$-C_6H_4$-4-$N(CH_3)_2$] showed the highest IC_{50} value for the three strains (IC_{50} values from 47 to 100 μM) (see Table 1).

In order to compare the activity of each compound regarding the three strains, the IC_{50} values, transformed into potency ($log1/IC_{50}$), were analyzed by ANOVA statistical test and post-hoc Tukey test (Fig. 3). The most active compound c20 showed distinct potency values for the three strains ($p < 0.001$; Fig. 3), being more active against the Y strain. On the other hand, compounds c2 [$-C_5H_{11}$], c6 [$-C_6H_{11}$] and c11 [$-C_8H_{17}$] presented the same activity values against the three strains ($p = 0.083$; $p = 0.473$, $p = 0.475$, respectively; Fig. 3). Since an ideal drug should be active against all types of *T. cruzi* strains, the reported findings can be considered quite interesting for developing novel promising agents against CD. The higher resistance of the Y strain against NFX ($log1/IC_{50} = 4.89$; $p < 0.001$), in comparison to the other two strains, was not observed for most of the compounds (Fig. 3). This suggests that the mode of action and/or the activation process of these compounds might differ from those/that of NFX.

2.3. Cytotoxicity assays

In order to evaluate the cytotoxicity of the compounds, assays were carried out using human fibroblast cells LL-24 (Table 2). Eight compounds (8/21; 36%) showed IC_{50} values lower than 200 μM, which was the maximum drug concentration used due to the solubility in the culture medium. The selectivity index (SI) was calculated by comparing the IC_{50} values obtained for *T. cruzi* strains and human cells (Table 2). Compounds c15 [$-C_6H_4$-4-C_4H_9], c19 [$-C_6H_4$-4-OC_4H_9], and c20 [$-C_6H_4$-4-C_6H_5] showed the highest SI values (Table 2).

2.4. Molecular modeling approach, descriptors calculation and variables selection

The three-dimensional (3D) molecular models of the compounds were constructed and energy-minimized as reported in the experimental section. The lowest-energy conformer of each compound was selected from the equilibrium region of the conformational ensemble profile (CEP) from molecular dynamics (MD) simulations (Fig. 1S, Supplementary Material). The root mean square deviation (RMSD) values were used as criterion in order to verify any change related to the atomic positions by performing the superimposition of each selected conformer from CEP (after

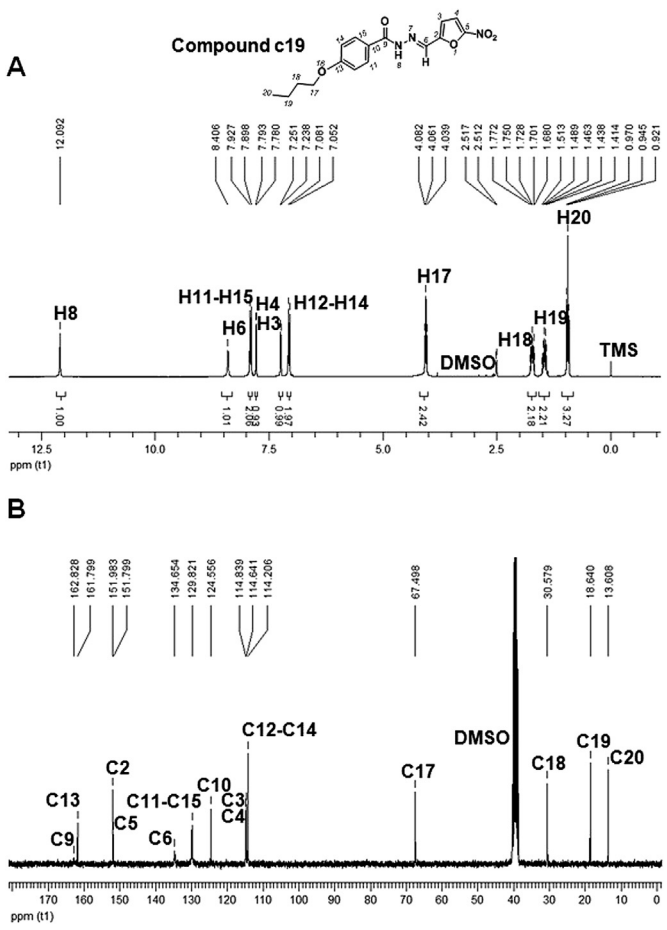

Fig. 2. NMR spectra of compound c19. (A) ^{1}H NMR (300 MHz/DMSO-d_6): chemical shifts of hydrogen's, H_6 and H_8, showing the formation of 5-nitrofuran derivatives; (B) ^{13}C NMR spectra (75 MHz/DMSO-d_6): chemical shifts of carbons, C_6 and C_9, indicating the formation of 5-nitrofuran derivatives.

simulation) and the corresponding energy-minimized structure. For small molecules, whose experimental coordinates (X-ray diffraction or NMR) are available, RMSD values higher than 0.1 Å indicate the structural arrangement was not maintained after calculation. Herein, however, part of the designed compounds scaffold was structurally different from NF, the lead compound. Then, conserved regions, as the 5-nitro-2-furan group (fragment related to the NF pharmacophoric group) and the *N*-acylhydrazone moiety, were taken into account to carry out the molecules' superimposition. The lowest-energy conformer more frequent from CEP was energy-minimized and, then, used as input to compute the molecular properties.

The total potential energy values and all intramolecular energy contribution values are among the calculated thermodynamic parameters for the set of compounds (Table 1S, Supplementary Material). Forty five descriptors, or molecular properties, of different nature (thermodynamic, hydrophobic, electronic, topological, geometric, and steric) were computed for each compound. The values of calculated descriptors and the respective methods used for calculation are shown in Table 2S (Supplementary Material). Thus, a table composed by 21 rows (samples or compounds) and 45 columns (independent variables or descriptors or molecular properties) was generated and used as input to perform the exploratory data analysis (PCA and HCA).

The biological data (anti-*T. cruzi* activity; $\log 1/IC_{50}$) corresponds to the dependent variable. Before running the exploratory data analysis, a preliminary variable selection was carried out. Each strain was considered in order to find relevant descriptors for each DTU activity. Two criteria, or filters, were used: the Pearson's linear correlation coefficient between descriptors and inhibitory activities (cut off value of 0.3), and visual inspection of scatter plots of biological activity ($\log 1/IC_{50}$ values) *versus* each calculated molecular property or descriptor [29]. The findings are presented in Fig. 2S (Supplementary Material). Regarding those filters, the following descriptors were selected: thermodynamic descriptor ($E_{TOT,}$ total potential energy; $E_{VDW,}$ van der Waals intramolecular energy contribution); electronic descriptors (μ, dipole moment; μ_x, component x of dipole moment); steric descriptor (ASA_h, solvent accessible surface area of all hydrophobic atoms) [37]; steric/geometric property ($SA_{vdW,}$ van der Waals surface of the molecule) [38]; calculated *n*-octanol/water partition coefficient ($ClogP_{WM}$) [39–41]; and topological descriptor (Wiener index, I_{Wiener}) [42].

A preliminary analysis provided the same descriptors or independent variables for the three strains: Y, Silvio X10 cl1, and Bug 2149 cl10; and, the final table was composed by 8 descriptors (columns) and 21 compounds (rows). Of note, the autoscaling procedure was applied as a preprocessing method [43], before running the exploratory analysis, due to the distinct magnitude orders among the calculated variables.

2.5. Exploratory data analysis

Exploratory data analysis comprises unsupervised multivariate methods as HCA and PCA [27,28]. The PCA and HCA findings were complementary, and are shown in Fig. 4. According to the factors selection (Fig. 4A), the first two factors, or PC, described 76.52% of total variance from the original data (PC1 = 58.10% and PC2 = 18.41%). Thus, the information of the two components, PC1 and PC2, was exploited more detailed.

The loading table (Fig. 4B) indicates descriptors that influenced more the compounds discrimination. In PC1, the descriptor ASA_h was more significant in describing the samples/compounds. Steric/geometric (SA_{vdW}), topological (I_{Wiener}) and hydrophobic ($ClogP_{WM}$) properties also presented high loadings values in PC1. In PC2, a thermodynamic property (van der Waals intramolecular energy contribution (E_{vdW})) presented the highest loading value. Moreover, electronic properties (μ_x and μ) were influenced more the discrimination process in PC2.

Regarding the scores plot (Fig. 4D), the compounds at the right side (positive values; inside the red square – group A) of PC1 were highly active against the three strains (c15 [$-C_6H_4$-4-C_4H_9], c18 [$-C_6H_4$-4-NC_4H_9], and c20 [$-C_6H_4$-4-C_6H_5]; moderately active: c12 [$-C_6H_4$-4-*iso*-C_3H_7],c13 [$-C_6H_4$-4-C_3H_7], c16 [$-C_6H_4$-4-*tert*-C_4H_9], c17 [$-C_6H_4$-4-OC_3H_7], c19 [$-C_6H_4$-4-OC_4H_9], and c21 [$-C_6H_4$-2-OC_6H_5]). The main similarity among these compounds is the presence of bulky substituent groups in their structure and the high values of ASA_h. This characteristic reinforces the high loadings values of steric, steric/geometric and topological properties in PC1, which explains 58.10% from the total variance of the original data. The compounds presenting low values of ASA_h and less bulky aryl, alkyl, and cicloalkyl substituent groups were grouped in the blue square group B (negative values; inside the blue square). In group B, it was also observed lower values of biological activity in comparison to most of the compounds in group A. In this analysis, exceptions were observed for c7 [$-C_6H_4$-3-CH_3], c11 [$-C_8H_{17}$], and c14 [$-C_6H_4$-4-$N(CH_3)_2$]. These compounds not only have similar steric, topological and steric/geometric properties in comparison to other compounds in group A, but also have moderate or low anti-*T. cruzi* activity. Compounds c7 [$-C_6H_4$-3-CH_3] and c14 [$-C_6H_4$-4-$N(CH_3)_2$] presented lower

ASA_h values in group A. Compound c14 [$-C_6H_4$-4-$N(CH_3)_2$], which presented the lowest activity against the three strains, was in group A because the steric similarities. The low activity for c14 was not clear, so far. Compound c14 presented higher value for the μ_x descriptor (component x of dipole moment; 7.86 Debye) as compared to the most active compounds c15, c18, and c20 ($\mu_x = -7.63$, -9.85 and -7.44 Debye, respectively). The negative loading value for μ_x (Fig. 4B) indicates an inverse structure–property relationship.

The dendrogram of the samples (HCA) (Fig. 4E) showed two main clusters: A (50.2% similarity) and B (38.8% similarity). Cluster A grouped the most active compounds which correspond to the compounds in the red square (score plot; Fig. 4D). The findings were complementary in both analysis, PCA and HCA. It is noteworthy that the most active compounds against the three strains, c15, c18 and c20, were grouped in the sub-cluster A and share 61.6% similarity. In cluster B are grouped the same compounds found in the blue square of the score plot. Compound c1 [$-CH_3$], the smallest molecule of the set, shares 38.8% similarity with compounds in the sub-clusters B′ and B″. Compounds containing aryl and less bulky substituent groups were grouped in sub-cluster B′ and share 69.4% similarity. In the sub-cluster B″ can be found compounds presenting alkyl and cicloalkyl substituent groups (0.62 similarity index). Thus, steric, steric/geometric and topological properties seemed to be responsible for the separation pattern obtained in HCA of samples (red and blue cluster).

The outliers' diagnosis plot (Fig. 4C), implemented in Pirouette 3.11 [44,45] was also performed through the Mahalanobis distance [46]. The sample residual threshold was based upon a ninety-five percent of confidence level interval set internally in Pirouette 3.11 [44]. The compounds did not exceed the considered threshold, meaning the calculated properties were sufficient to describe the structural features of the entire data set.

In order to visualize the steric property, such as solvent accessible surface area of hydrophobic atoms (ASA_h; $|q_i| < 0.125$) [37], which was pointed out in the exploratory analysis, some compounds where chosen. Better anti-*T. cruzi* activity seems to be related to higher values of ASA_h descriptor (Fig. 5). The most active compounds, c20 and c18, showed high ASA_h values, whereas the non-active compound, c14, and c9 and c1 showed low ASA-h values.

3. Conclusions

A set of twenty one 5-nitro-2-furfuriliden derivatives was designed and synthesized. Molecular modifications were based on the influence of physicochemical properties, mainly hydrophobicity and steric/hydrophobic properties. The trypanocidal activity was determined *in vitro* against epimastigote forms of divergent *T. cruzi* strains, belonging to DTUs more prevalent in CD patients. The *N*′-[(5-nitrofuran-2-yl) methylene] substituted hydrazides have presented IC_{50} values from 3 to 250-fold lower than the lead compound NF ($IC_{50} = 300$ μM). Except to compound c14, all derivatives showed enhanced trypanocidal activity against the three strains in comparison to BZD, the most widely used drug for CD treatment. Regarding the Y strain, around 62% of the compounds were more active than NFX. Compound c20 [$-C_6H_4$-4-C_6H_5] was the most active against the three strains (IC_{50} values from 1.17 to 3.17 μM); followed by compounds c15 [$-C_6H_4$-4-C_4H_9], c18 [$-C_6H_4$-4-NC_4H_9], and c19 [$-C_6H_4$-4-OC_4H_9]. Conversely, compound c14 [$-C_6H_4$-4-$N(CH_3)_2$] has showed the highest IC_{50} value for the three strains (IC_{50} values from 47 to 100 μM). Cytotoxicity assays using human fibroblast cells demonstrated high selectivity indices for several compounds.

HCA and PCA findings were complementary, and suggested that topological, steric/geometric and electronic properties are primarily responsible for the compounds discrimination, and for the anti-*T. cruzi* activity, as well.

As the next step of our studies, the most promising compounds found here will be evaluated against intracellular amastigote forms, since they are encountered in the mammalian host.

Table 1
Biological activity of 5-nitro-2-furfuriliden derivatives against epimastigote forms of Y, Silvio X10 cl1, and Bug 2149 cl10 strains.

Compounds	Y		Silvio X10 cl1		Bug 2149 cl10	
	IC_{50} (μM) (mean ± SD)	$\log 1/IC_{50}$	IC_{50} (μM) (mean ± SD)	$\log 1/IC_{50}$	IC_{50} (μM) (mean ± SD)	$\log 1/IC_{50}$
c1	13.72 ± 0.21	4.86	27.14 ± 2.90	4.57	15.85 ± 2.24	4.80
c2	10.24 ± 1.04.	4.99	9.72 ± 099	5.01	12.20 ± 1.33	4.91
c3	11.88 ± 1.19	4.93	19.92 ± 1.76	4.70	14.55 ± 1.26	4.84
c4	9.41 ± 0.90	5.03	13.85 ± 1.34	4.86	12.25 ± 1.06	4.91
c5	12.64 ± 0.55	4.90	31.10 ± 2.21	4.51	14.25 ± 1.25	4.85
c6	14.42 ± 1.50	4.84	13.67 ± 1.77	4.86	12.77 ± 1.34	4.89
c7	9.89 ± 1.00	5.00	27.69 ± 2.53	4.56	24.81 ± 2.68	4.61
c8	10.98 ± 1.10	4.96	20.24 ± 1.24	4.69	12.26 ± 1.01	4.91
c9	23.06 ± 1.72	4.64	37.42 ± 2.69	4.43	25.26 ± 1.41	4.60
c10	9.15 ± 0.95	5.04	19.98 ± 1.75	4.70	14.45 ± 1.18	4.84
c11	13.49 ± 0.93	4.87	14.73 ± 1.50	4.83	14.40 ± 1.13	4.84
c12	3.91 ± 0.33	5.41	6.09 ± 0.67	5.22	9.04 ± 0.49	5.04
c13	9.09 ± 0.53	5.04	10.28 ± 0.36	4.99	9.80 ± 0.39	5.01
c14	100.00 ± 6.87	4.00	100.00 ± 5.27	4.00	47.29 ± 2.99	4.33
c15	3.10 ± 0.29	5.51	4.75 ± 0.36	5.32	4.41 ± 0.46	5.36
c16	9.43 ± 1.00	5.03	13.65 ± 1.05	4.86	13.67 ± 1.40	4.86
c17	7.33 ± 0.47	5.13	12.78 ± 0.62	4.89	9.72 ± 0.56	5.01
c18	3.39 ± 0.31	5.51	4.34 ± 0.33	5.36	4.22 ± 0.49	5.37
c19	3.47 ± 0.20	5.46	5.07 ± 0.28	5.29	4.25 ± 0.40	5.37
c20	1.17 ± 0.12	5.93	3.17 ± 0.32	5.50	1.81 ± 0.18	5.74
c21	7.79 ± 0.80	5.11	12.34 ± 0.18	4.91	12.19 ± 1.06	4.91
BZD	40.40 ± 3.37	4.39	29.16 ± 2.90	4.54	30.63 ± 3.00	4.51
NFX	12.84 ± 1.30	4.89	6.02 ± 0.32	5.22	7.32 ± 0.76	5.14
NF	300.00 ± 5.12	3.52	ND	–	300.00 ± 9.32	3.52

IC_{50} values are presented as mean and the standard deviation (SD) corresponds to triplicates from at least two independent experiments. Errors are in a range of 10%. $\log 1/IC_{50}$ values represent the biological activity in potency (molar concentration); BZD, Benznidazole; NFX, Nifurtimox; NF, Nifuroxazide; ND: not determined. NF did not show any anti-*T. cruzi* activity in Silvio X10 cl1 strain probably because solubility conditions.

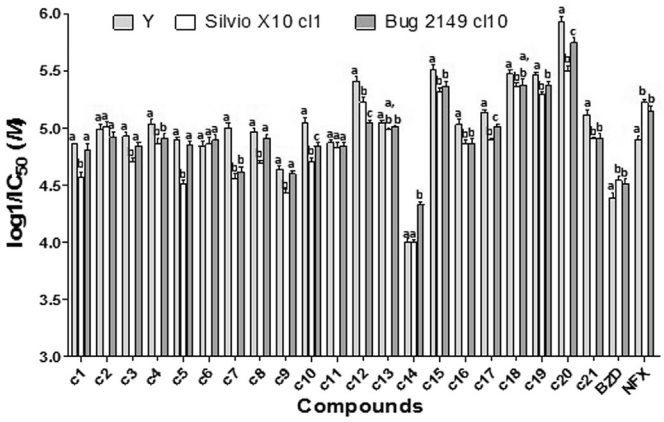

Fig. 3. Biological activity ($log1/IC_{50}$) of 5-nitro-2-furfuriliden derivatives against epimastigote forms of Y, Silvio X10 cl1, and Bug 2149 cl10 strains. Data were analyzed through statistical test ANOVA and post-hoc test Tukey ($p < 0.005$). Letters denote differences between strains for the same compound. Compounds c1, c5, c7, c8, c9, c10, c12, c14, c17, c20 and NFX, $p < 0.001$; c2 $p = 0.008$; c3 $p = 0.001$; c4 $p = 0.006$; c6 $p = 0.473$; c11 $p = 0.475$; c13 $p = 0.042$; c15 $p = 0.003$; c16 $p = 0.005$; c18 $p = 0.038$; c19 $p = 0.002$; c21 $p = 0.001$; and BZD $p = 0.011$. Confidence interval was 95%. BZD, Benznidazole; NFX, Nifurtimox.

4. Experimental sections

4.1. Chemistry

NMR spectra were recorded on a Bruker ADPX Advanced (300 MHz) spectrometer employing DMSO-d_6 solutions with tetramethylsilane as internal standard. Melting points were determined using Büchi M-560 apparatus, and elemental analysis was performed on a Perkin–Elmer 24013 CHN Elemental Analyzer.

4.1.1. General procedure for the synthesis of hydrazides

each carboxylic acid (a) (0.02 mol) was refluxed for 4 h in 20.0 mL (0.49 mol) of anhydrous methanol and 0.5 mL (0.01 mol) of sulfuric acid. The reaction mixture was cooled down to room temperature and the hydrazine hydrate 80% (v/v) (10.0 mL, 0.13 mol) was added. The system was maintained by vigorously stirring for more 30 min in reflux. After this period, the mixture was maintained at low temperature to give (b), and was purified from ethyl acetate. The hydrazide intermediate of compounds 1 and 2 were commercially obtained (Sigma–Aldrich, purity of 97%) [47].

4.1.2. General procedure for the synthesis of nitrofurans compounds (c1–c21)

compounds were synthesized by refluxing 5-nitro-2-furaldehyde 98% (5 mmol) and hydrazides (b) (5 mmol) in water, sulfuric acid, acetic acid, and methanol (8:7:8:20 v/v) for 1 h. After cooling, the mixture was poured into cold water to precipitate, and recrystallized from acetonitrile [33]. Compounds highly water soluble were synthesized in 10 mL of ethanol PA (5 mmol) with 5-nitro-2-furaldehyde 98% (1 mmol) and hydrazides (b) (1 mmol), at room temperature, and vigorous stirring for 6–8 h. (see structural elucidation in Supplementary Material) [34]. The compound c21 [$-C_6H_4$-2-OC_6H_5] was identified as a new chemical entity and is described as follows.

4.1.2.1. N′-[(5-Nitrofuran-2-yl) methylene]-2-phenoxybenzohydrazide (c21). Yellow solid (74%); mp 197.0–198.0 °C. 1H NMR (DMSO-d6, 300 MHz): δ (ppm): 12.14 (s, 1H, H8), 8.30 (s, 1H, H6), 7.77 (d, 1H, J = 3.6 Hz, H4), 7.69 (d, 1H, J = 7.7 Hz, H11), 7.56–7.37 (m, 3H, H12, H13, H14), 7.32–7.23 (m, 2H, H18, H20), 7.17–6.97 (m, 4H, H3, H17, H19, H21); 13C NMR {H} (DMSO-d6, 75 MHz): δ (ppm): 169.5/162.4 (C9), 156.4 (C16), 153.9 (C15), 151.9 (C2), 151.6 (C5), 135.3 (C13), 132.3/130.0 (C6), 126.7 (C11), 123.7 (C18, C20), 122.9 (C12, C19), 119.0 (C10), 118.6 (C17, C21), 117.5 (C14), 115.3 (C4), 114.5 (C3); Anal. Calcd. for (C18H13N3O5): C, 61.54; H, 3.73; N, 11.96. Found: C, 61.54; H, 3.72; N, 12.18.

4.2. Anti-T. cruzi activity assay

The activity of the compounds was determined against *T. cruzi* epimastigote forms of the Y, Silvio X10 cl1, and Bug 2149 cl10 strains

Table 2
Cytotoxicity of 5-nitro-2-furfuriliden derivatives, benznidazole, nifurtimox and nifuroxazide against LL-24 human fibroblast cells and their respective selectivity index.

Compounds	LL-24 cells IC_{50} (μM) (mean)	Y		Silvio X10 cl1		Bug 2149 cl10	
		IC_{50} (μM) (mean ± SD)	SI	IC_{50} (μM) (mean ± SD)	SI	IC_{50} (μM) (mean ± SD)	SI
c1	>200	13.72 ± 0.21	>15	27.14 ± 2.90	>7	15.85 ± 2.24	>13
c2	99	10.24 ± 1.04	10	9.72 ± 099	10	12.20 ± 1.33	8
c3	58	11.88 ± 1.19	5	19.92 ± 1.76	3	14.55 ± 1.26	4
c4	>200	9.41 ± 0.90	>21	13.85 ± 1.34	>14	12.25 ± 1.06	>16
c5	178	12.64 ± 0.55	14	31.10 ± 2.21	5.72	14.25 ± 1.25	12.49
c6	>200	14.42 ± 1.50	>14	13.67 ± 1.77	>15	12.77 ± 1.34	>16
c7	>200	9.89 ± 1.00	>20	27.69 ± 2.53	>7	24.81 ± 2.68	>8
c8	97	10.98 ± 1.10	8.83	20.24 ± 1.24	4.79	12.26 ± 1.01	7.91
c9	>200	23.06 ± 1.72	>9	37.42 ± 2.69	>5	25.26 ± 1.41	>8
c10	187	9.15 ± 0.95	20.45	19.98 ± 1.75	9.36	14.45 ± 1.18	12.94
c11	91	13.49 ± 0.93	7	14.73 ± 1.50	6	14.40 ± 1.13	6
c12	>200	3.91 ± 0.33	>51	6.09 ± 0.67	>33	9.04 ± 0.49	>22
c13	89	9.09 ± 0.53	10	10.28 ± 0.36	9	9.80 ± 0.39	9
c14	>200	100.00 ± 6.87	>2	100.00 ± 5.27	>2	47.29 ± 2.99	>4
c15	>200	3.10 ± 0.29	>64	4.75 ± 0.36	>42	4.41 ± 0.46	>45
c16	>200	9.43 ± 1.00	>21	13.65 ± 1.05	>15	13.67 ± 1.40	>15
c17	>200	7.33 ± 0.47	>27	12.78 ± 0.62	>16	9.72 ± 0.56	>21
c18	47	3.39 ± 0.31	14	4.34 ± 0.33	11	4.22 ± 0.49	11
c19	>200	3.47 ± 0.20	>58	5.07 ± 0.28	>39	4.25 ± 0.40	>47
c20	>200	1.17 ± 0.12	>176	3.17 ± 0.32	>63	1.81 ± 0.18	>110
c21	>200	7.79 ± 0.80	>26	12.34 ± 0.18	>16	12.19 ± 1.06	>16
BZD	>200	40.40 ± 3.37	>5	29.16 ± 2.90	>7	30.63 ± 3.00	>6
NFX	>200	12.84 ± 1.30	>16	6.02 ± 0.32	>33	7.32 ± 0.76	>27
NF	>200	300.00 ± 5.12	>1	ND	–	300.00 ± 9.32	>1

IC_{50} values are presented as mean, and the standard deviation (SD) corresponds to triplicates from at least two independent experiments. Errors are in a range of 10%. SI: selectivity index (SI = IC_{50} of cell line/IC_{50} of *T. cruzi*). BZD, Benznidazole; NFX, Nifurtimox; NF, Nifuroxazide (lead-compound); ND: not determined.

[6]. Epimastigotes were cultured in Liver Infusion-Tryptose (LIT) medium with 10% fetal calf serum (FCS) at 28 °C. Exponentially growing epimastigotes (10^7 parasites/mL) were incubated in 96-well, flat-bottom tissue culture plates in 200 μL LIT-FCS medium with different drug concentrations for 72 h at 28 °C. DMSO was added to the medium in a concentration that would not exceed 1.0% in order to solubilize the compounds and reference drugs. DMSO concentration used herein had no effect on epimastigote growth. After the incubation period, the amount of viable parasites was determined as previously described [36], in a microplate reader (Biochrom – EX Read 400, England), at 562 nm wavelength. The anti-*T. cruzi* activity was calculated by using the formula: $PGI = \{1 - [(A_p - A_{pb})/(A_c - A_{cb})]\} \times 100$, where: PGI = percentage of growth inhibition; $A_p = A_{562}$ of the epimastigote culture at a given compound concentration after 72 h incubation; $A_{pb} = A_{562}$ of the medium at a given compound concentration without parasites (blank of compounds in each concentration); $A_c = A_{562}$ of the epimastigote culture in the absence of any compound; $A_{cb} = A_{562}$ of the LIT-FCS medium (blank). At least two independent assays with three replicates in each assay were performed. The inhibitory concentration IC_{50}, corresponding to the drug concentration that inhibited 50% parasite growth, was determined from the percentage of growth inhibition provided by at least five drug concentrations, employing the nonlinear model growth/sigmoid dose–response (Origin Pro 8.0 software) [48].

4.3. Cytotoxicity assays

Cell culture of LL-24 human fibroblast cells were maintained in RPMI 1640 containing 10% FBS, 100 UI penicillin and 100 μg/ml gentamycin at 37 °C in 95% air and 5% CO_2. LL-24 cells were plated in triplicate in 96-well microplates at $1*10^4$ cells/well density into flat microtiter plates, and incubated overnight at 37 °C in a humidified incubator containing 5% CO_2. Then, the cells were treated with the compounds from 12.5 to 200 μM in a final volume of 100 μL. After 24 h treatment, cells were exposed to 5 mg/mL 3-[4,5-dimethylthiazol-2-yl]-2,5-diphenyl-tetrazolium bromide (MTT) for 2 h, and the precipitated formazan was dissolved in 0.1 N HCl in isopropanol, and measured at 540 nm with a microplate reader Thermo Plate (Thermoplate TP Reader, Tokay Hit, Japan). The IC_{50} values were determined from the percentage of inhibition growth using nonlinear model growth/sigmoid dose–response (Origin Pro 8.0 program) [48] for each case using, at least, five concentration values. Cytotoxicity percentages (% C) were determined as follows: $\%\ C = 100 - [(OD_d - OD_{dm})/(OD_c - OD_{cm}) \times 100]$, where OD_d is the mean of OD_{595} of wells with macrophages and different

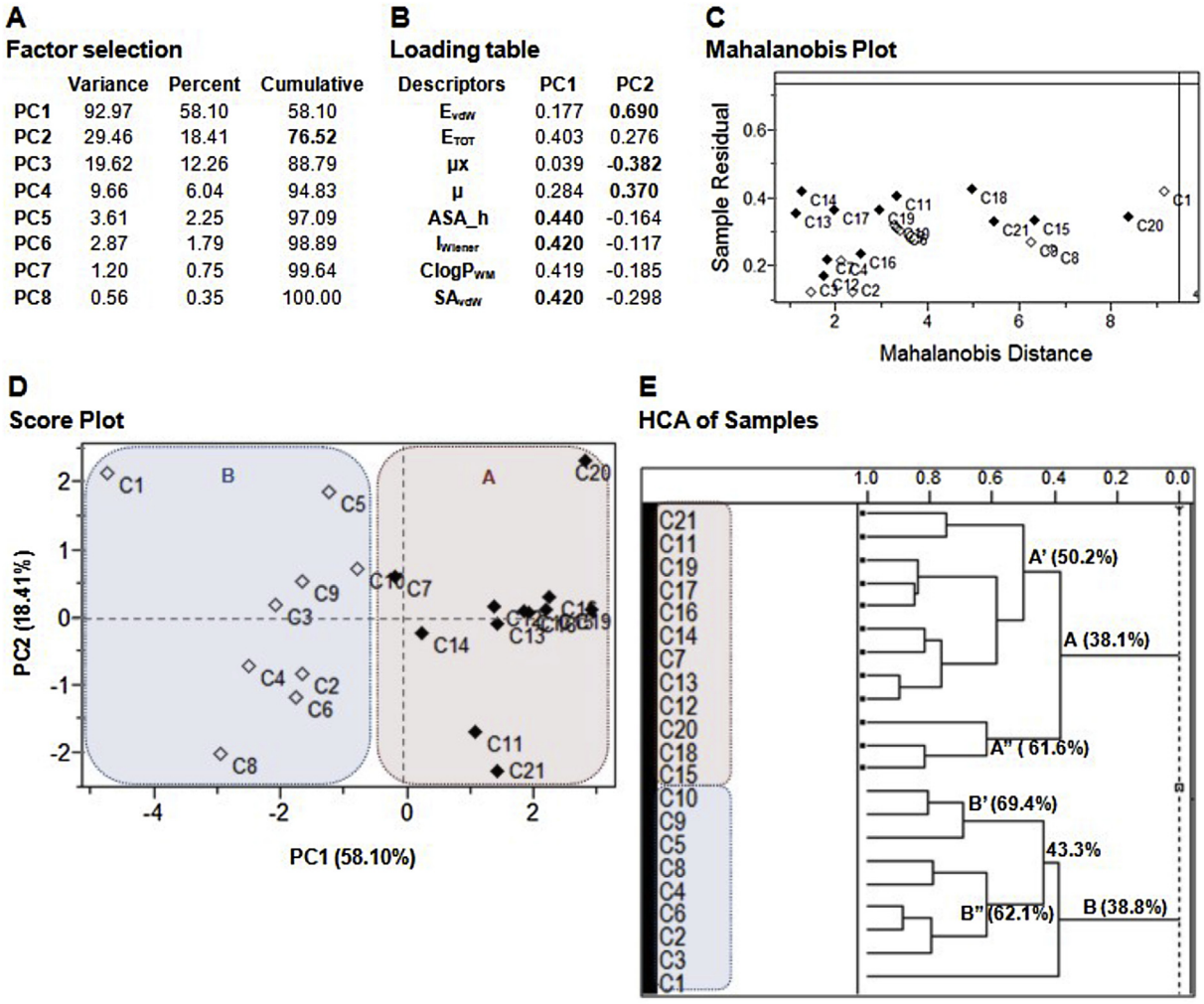

	Variance	Percent	Cumulative
PC1	92.97	58.10	58.10
PC2	29.46	18.41	**76.52**
PC3	19.62	12.26	88.79
PC4	9.66	6.04	94.83
PC5	3.61	2.25	97.09
PC6	2.87	1.79	98.89
PC7	1.20	0.75	99.64
PC8	0.56	0.35	100.00

Descriptors	PC1	PC2
E_{vdW}	0.177	**0.690**
E_{TOT}	0.403	0.276
μx	0.039	**-0.382**
μ	0.284	**0.370**
ASA_h	**0.440**	-0.164
I_{Wiener}	**0.420**	-0.117
$ClogP_{WM}$	0.419	-0.185
SA_{vdW}	**0.420**	-0.298

Fig. 4. PCA and HCA findings. (A) PCA factors selection: the two first PC explained 76.52% of total variance from the original data; (B) Loadings' table for the two first PC, PC1 and PC2: high loadings values are in bold; (C) Outliers' diagnosis: sample residual *versus* Mahalanobis distance; (D) PCA scores' plot for PC1 *versus* PC2; (E) Dendrogram of samples (HCA).

concentrations of the compounds; OD_{dm} is the mean of OD_{595} of wells with different compounds concentration in the medium; OD_c is the growth control and OD_{cm} is the mean of OD_{595} of wells with medium only.

4.4. Molecular modeling approach, calculation and selection of descriptors

The 3D molecular models of the compounds were built up using as reference geometry the Cartesian coordinates of NF crystallographic structure (LEQTAC code, $R_{factor} = 0.11$) [49], retrieved from Cambridge Structural Database (CSD) [50]. For the reference drugs molecular models, The 3D molecular models of reference drugs were constructed using the Cartesian coordinates of both, BZD ($R_{factor} = 0.025$) [51] and NFX analog ($R_{factor} = 0.042$) [52], as template. Each molecular model was energy-minimized in MM + force field [53], without any constrains. The partial atomic charges were calculated employing the AM1 (Austin Model 1) semiempirical method [54]. Energy minimization was also performed employing the MOLSIM 3.2 program [55], employing the steepest descent and, subsequently, the conjugated gradient method. The convergence criterion was set up as 0.01 kcal/mol. The energy-minimized structures were the input to MD simulations of 1ns (1,000,000 steps; step size of 1fs) at 301 K (28 °C), the same temperature of biological assay. Dielectric constant of 3.5 was used to simulate the environment of the biological membranes and enzymes' interaction sites (2–5). It was assigned a fictitious atomic mass of 5000 u.m.a. to atoms in the conserved scaffold (based on ^{1}H and ^{13}C NMR spectra, and NF crystallized structure) in order to maintain the structural integrity during calculation. Trajectory files were recorded every 20 simulation steps to generate 50,000 conformations. The lowest-energy conformation was selected from the equilibrium region of conformational ensemble profile (CEP) and compared (superimposed; Hyperchem 8.0) [56] to the initial energy-minimized molecular model to verify whether the structural integrity was maintained after simulation. RMSD (root-mean square deviation) values were used as criterion based on superimposition data. After energy-minimized, the selected conformer of each compound was used to compute molecular properties of different nature employing different software. The thermodynamic properties were obtained by performing MD simulation. The intramolecular energy contribution of solvation was calculated using the hydration shell model proposed by Forsythe and Hopfinger (1973) [57].

ClogP values were calculated using the method available in Sybyl 8.0, Ghose et al., 1998-SLN ($ClogP_{SG\text{-}SLN}$) [39]. Marvin 5.2.1_1 program [41] was used to compute steric, topological/geometric, and lipophilic properties. The ClogP values ($ClogP_{WM}$) were calculated by the weighted method, assigning equal weight for each method [40,58,59]. The ASA values were computed using the solvent radius (1.4 Å, water molecule). The solvent accessible surface area was visualized for the most active compounds and reference drugs using the ViewerLite 5.0 program [60]. In addition, molecular properties related to the substituent groups were retrieved from previous report [61]. Further detailed information regarding all descriptors, methods, and respective software used to perform calculations are listed in Table 3S (Supplementary Material).

Then, a table containing 45 columns (independent variables, or descriptors, plus biological activity, $log1/IC_{50}$) and 21 rows (number of compounds) was generated, and the selection of variables was previously carried out. Two criteria or filters were considered: (i) the Pearson correlation coefficient, and (ii) a visual inspection of scatter plots correlating biological activity and each descriptor, or molecular property [29]. The Pearson correlation coefficient value of 0.3 was formerly used as cut off for selecting the calculated independent variables. Regarding the visual inspection, only variables presenting uniform distribution with the biological data were selected to compose the final table. The final table was used as input to perform the exploratory data analysis. Because of magnitude orders differences among the calculated variables, the autoscaling procedure was applied as a preprocessing method [43].

4.5. Exploratory data analysis (HCA and PCA) [29, 30]

Exploratory data analysis was carried out using Pirouette 3.11 [44]. Hierarchical clustering analysis, HCA, was performed employing the complete linkage method and Euclidean distance [29,30,44]. Distances between pairs of samples (or variables) are calculated and compared in HCA. Samples are considered similar when the distances between them are relatively small. The calculated distances between samples are set on a similarity matrix whose elements are called similarity indices, ranging between 0 and 1, where 1 is equivalent to a maximum similarity. The results are usually presented as a two-dimensional chart, called

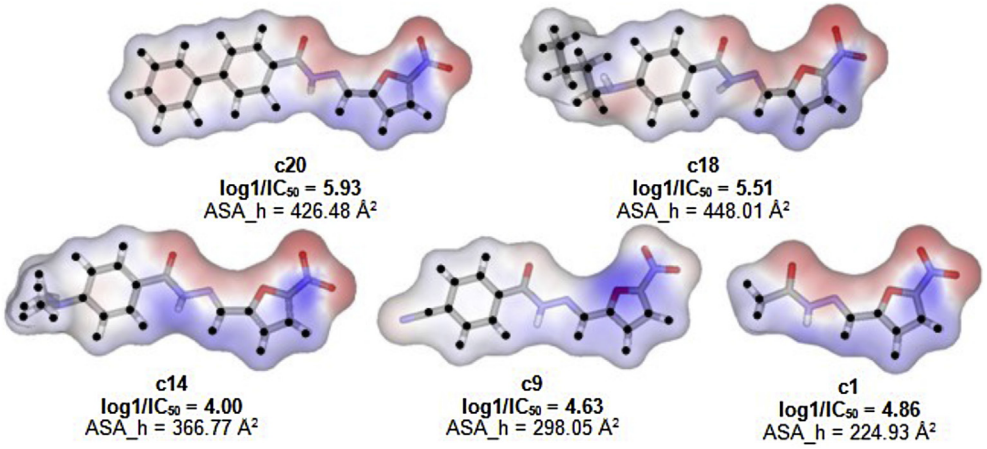

Fig. 5. Visualization of ASA_h descriptor for compounds c1, c9, c18 and c20. ASA_h was calculated using ViewerLite 5.0 (1.4 Å radii), and displayed as transparent format. Black spots correspond to hydrophobic atoms ($|q_i| < 0.125$; $|q_i|$ is the absolute value of the partial charge of the atom). The compounds are showed in stick model (carbon atoms in gray, oxygen in red, nitrogen in blue, sulfur in yellow, and hydrogen atoms are shown in white). (For interpretation of the references to colour in this figure legend, the reader is referred to the web version of this article.)

dendrogram [44].

The multivariate distance d_{ab} between two samples vectors, a and b, was determined by computing differences at each of the m variables:

$$d_{ab} = \left[\sum_{i}^{m}\left(x_{aj} - x_{bj}\right)^{M}\right]^{1/M}$$

M is the order of the distance, and here corresponds to the Euclidean distance (M = 2) [44]. Because of inter-sample distances can vary with the type and number of measurements, it is customary to transform them onto a somewhat more standard scale of similarity, where d_{max} is the largest distance in the data set:

$$\text{similarity}_{ab} = 1 - \frac{d_{ab}}{d_{max}}$$

Regarding principal components analysis, PCA, the data were decomposed into two matrices, one of scores related to the samples, and another of loadings, related to the variables [29,30]. The new set of axes generates the principal components (PC), or factors, into which are the information related to the original descriptors. Thus, the number of PC that explain most of the variability in the data set can be determined, considering that these PC are uncorrelated and mutually orthogonal variables built up as simple linear combinations from the original data [29,30]. Herein, PCA was run up to eight factors, or PC. The outliers' diagnosis, implemented in Pirouette 3.11 software [44], was also performed through the Mahalanobis distance [62].

Acknowledgments

The authors thank Dr. José Alexandre Marzagão Barbuto of Immunology Department of Biomedical Sciences Institute of University of São Paulo for the availability of his laboratory for the cytotoxicity assays. The authors also thank Dr. Maria Júlia M. Alves (Department of Biochemistry, Institute of Chemistry, University of São Paulo) for providing the Y strain of *T. cruzi* and LIT medium and Bayer Schering Pharma AG for the kind donation of Nifurtimox (Lampit).

This work was supported by grants of Fundação de Amparo à Pesquisa do Estado de São Paulo (FAPESP) (grant number 2013/13333-8 and 2014/06061-4) and Conselho Nacional de Desenvolvimento Científico e Tecnológico (CNPq) (grant number 304793/2009-4).

Appendix A. Supplementary data

Supplementary data related to this article can be found at http://dx.doi.org/10.1016/j.ejmech.2015.03.066.

References

[1] A. Rassi Jr., A. Rassi, J. Marcondes de Rezende, American trypanosomiasis (Chagas disease), Infect. Dis. Clin. N. Am. 26 (2012) 275–291.
[2] WHO, Technical Report Series, Research Priorities for Chagas Disease, Human African Trypanosomiasis and Leishmaniasis. Number 975, WHO, Geneva, 2012. http://apps.who.int/iris/bitstream/10665/77472/1/WHO_TRS_975_eng.pdf.
[3] O. Yun, M.A. Lima, T. Ellman, W. Chambi, S. Castillo, L. Flevaud, P. Roddy, F. Parreño, P.A. Viñas, P.P. Palma, Feasibility, drug safety, and effectiveness of etiological treatment programs for Chagas disease in Honduras, Guatemala, and Bolivia: 10-year experience of Médecins Sans Frontières, PLoS Negl. Trop. Dis. 3 (2009) e488.
[4] L.S. Filardi, Z. Brener, Susceptibility and natural resistance of *Trypanosoma cruzi* strains to drugs used clinically in Chagas disease, Trans. R. Soc. Trop. Med. Hyg. 81 (1987) 755–759.
[5] S.M. Murta, R.T. Gazzinelli, Z. Brener, A.J. Romanha, Molecular characterization of susceptible and naturally resistant strains of *Trypanosoma cruzi* to benznidazole and nifurtimox, Mol. Bioch. Paras. 93 (1998) 203–214.
[6] B. Zingales, S.G. Andrade, M.R.S. Briones, D.A. Campbell, E. Chiari, O. Fernandes, F. Guhl, E. Lages-Silva, A.M. Macedo, C.R. Machado, A new consensus for Trypanosoma cruzi intraspecific nomenclature: second revision meeting recommends TcI to TcVI, Mem. Inst. Oswaldo Cruz. 104 (2009) 1051–1054.
[7] M. Miles, M. Llewellyn, M. Lewis, M. Yeo, R. Baleela, S. Fitzpatrick, M. Gaunt, I. Mauricio, The molecular epidemiology and phylogeography of Trypanosoma cruzi and parallel research on leishmania: looking back and to the future, Parasitology 136 (2009) 1509–1528.
[8] F. Guhl, J.D. Ramírez, *Trypanosoma cruzi* I diversity: towards the need of genetic subdivision? Acta Trop. 119 (2011) 1–4.
[9] B. Zingales, M.A. Miles, D.A. Campbell, M. Tibayrenc, A.M. Macedo, M.M. Teixeira, A.G. Schijman, M.S. Llewellyn, E. Lages-Silva, C.R. Machado, The revised *Trypanosoma cruzi* subspecific nomenclature: rationale, epidemiological relevance and research applications, Infect. Genet. Evol. 12 (2012) 240–253.
[10] D. Villarreal, C. Barnabé, D. Sereno, M. Tibayrenc, Lack of correlation between in vitro susceptibility to benznidazole and phylogenetic diversity of *Trypanosoma cruzi*, the agent of Chagas disease, Exp. Parasitol. 108 (2004) 24–31.
[11] M. Moreno, D.A. D'ávila, M.N. Silva, L. Galvão, A.M. Macedo, E. Chiari, E.D. Gontijo, B. Zingales, Trypanosoma cruzi benznidazole susceptibility in vitro does not predict the therapeutic outcome of human Chagas disease, Mem. Inst. Oswaldo Cruz. 105 (2010) 918–924.
[12] F.S. Buckner, J.A. Urbina, Recent developments in sterol 14-demethylase inhibitors for Chagas disease, Int. J. Parasitol. Drugs Drug Resist. 2 (2012) 236–242.
[13] I. Molina, J. Gómez i Prat, F. Salvador, B. Treviño, E. Sulleiro, N. Serre, D. Pou, S. Roure, J. Cabezos, L. Valerio, Randomized trial of posaconazole and benznidazole for chronic chagas' disease, New. Engl. J. Med. 370 (2014) 1899–1908.
[14] Drugs for Neglected Diseases Initiative. Proof of Concept Study of E1224 to Treat Adults Patients with Chagas Disease. in: ClinicalTrials.gov [Internet]. Bethesda (MD): National Library of Medicine (US). Available from: http://clinicaltrials.gov/ct2/show/NCT01489228?term=chagas+disease&rank=9. Identifier NCT 01489228.
[15] B. Zingales, M.A. Miles, C.B. Moraes, A. Luquetti, F. Guhl, A.G. Schijman, I. Ribeiro, Drug discovery for Chagas disease should consider Trypanosoma cruzi strain diversity, Mem. Inst. Oswaldo Cruz. 109 (6) (2014) 828–833.
[16] S.D. Jorge, A. Masunari, C.O. Rangel-Yagui, K.F.M. Pasqualoto, L.C. Tavares, Design, synthesis, antimicrobial activity and molecular modeling studies of novel benzofuroxan derivatives against *Staphylococcus aureus*, Bioorg. Med. Chem. 17 (2009) 3028–3036.
[17] S.D. Jorge, F. Palace-Berl, K.F. Mesquita Pasqualoto, M. Ishii, A.K. Ferreira, C.M. Berra, R.V. Bosch, D.A. Maria, L.C. Tavares, Ligand-based design, synthesis, and experimental evaluation of novel benzofuroxan derivatives as anti- *Trypanosoma cruzi* agents, Eur. J. Med. Chem. 64 (2013) 200–214.
[18] F. Palace-Berl, S.D. Jorge, K.F.M. Pasqualoto, A.K. Ferreira, D.A. Maria, R.R. Zorzi, L. de Sá Bortolozzo, J.Â.L. Lindoso, L.C. Tavares, 5-nitro-2-furfuriliden derivatives as potential anti- *Trypanosoma cruzi* agents: design, synthesis, bioactivity evaluation, cytotoxicity and exploratory data analysis, Bioorg. Med. Chem. 21 (2013) 5395–5406.
[19] C. Viodé, N. Bettache, N. Cenas, R.L. Krauth-Siegel, G. Chauvière, N. Bakalara, J. Périé, Enzymatic reduction studies of nitroheterocycles, Biochem. Pharmacol. 57 (1999) 549–557.
[20] R.R. Zorzi, S.D. Jorge, F. Palace-Berl, K.F.M. Pasqualoto, L. de Sá Bortolozzo, A.M. de Castro Siqueira, L.C. Tavares, Exploring 5-nitrofuran derivatives against nosocomial pathogens: synthesis, antimicrobial activity and chemometric analysis, Bioorg. Med. Chem. 22 (2014) 2844–2854.
[21] R. Docampo, Sensitivity of parasites to free radical damage by antiparasitic drugs, Chem-Biol. Interact. 73 (1990) 1–27.
[22] M. Boiani, L. Piacenza, P. Hernández, L. Boiani, H. Cerecetto, M. González, A. Denicola, Mode of action of nifurtimox and *N*-oxide-containing heterocycles against *Trypanosoma cruzi*: is oxidative stress involved? Biochem. Pharmacol. 79 (2010) 1736–1745.
[23] S.R. Wilkinson, C. Bot, J.M. Kelly, B.S. Hall, Trypanocidal activity of nitroaromatic prodrugs: current treatments and future perspectives, Curr. Top. Med. Chem. 11 (2011) 2072–2084.
[24] G. Priotto, S. Kasparian, W. Mutombo, D. Ngouama, S. Ghorashian, U. Arnold, S. Ghabri, E. Baudin, V. Buard, S. Kazadi-Kyanza, Nifurtimox-eflornithine combination therapy for second-stage African *Trypanosoma brucei gambiense* trypanosomiasis: a multicentre, randomised, phase III, non-inferiority trial, Lancet 374 (2009) 56–64.
[25] C. Lipinski, F. Lombardo, B. Dominy, P. Feeney, Experimental and computational approaches to estimate solubility and permeability in drug discovery and development settings, Adv. Drug Deliv. Rev. 23 (1997) 3–25.
[26] C.A. Lipinski, F. Lombardo, B.W. Dominy, P.J. Feeney, Experimental and computational approaches to estimate solubility and permeability in drug discovery and development settings, Adv. Drug Deliv. Rev. 64 (2012) 4–17.
[27] A.K. Ghose, V.N. Viswanadhan, J.J. Wendoloski, A knowledge-based approach in designing combinatorial or medicinal chemistry libraries for drug discovery. 1. a qualitative and quantitative characterization of known drug databases,, J. Comb. Chem. 1 (1999) 55–68.
[28] D.F. Veber, S.R. Johnson, H.-Y. Cheng, B.R. Smith, K.W. Ward, K.D. Kopple,

Molecular properties that influence the oral bioavailability of drug candidates, J. Med. Chem. 45 (2002) 2615–2623.
[29] M. Ferreira, Multivariate QSAR, J. Braz. Chem. Soc. 13 (2002) 742–753.
[30] K.R. Beebe, R.J. Pell, M.B. Seasholtz, Chemometrics: a Practical Guide, Wiley-Interscience, New York, 1998.
[31] H. Kubinyi, QSAR: Hansch Analysis and Related Approaches, VCH, New York, 1993.
[32] S.D. Jorge, F. Palace-Berl, A. Masunari, C.A. Cechinel, M. Ishii, K.F.M. Pasqualoto, L.C. Tavares, Novel benzofuroxan derivatives against multidrug-resistant *Staphylococcus aureus* strains: design using Topliss' decision tree, synthesis and biological assay, Bioorg. Med. Chem. 19 (2011) 5031–5038.
[33] L.C. Tavares, T.C. Penna, A.T. Amaral, Synthesis and biological activity of nifuroxazide and analogs, Boll. Chim. Farm. 136 (1997) 244–249.
[34] C.F. Da Costa, A.C. Pinheiro, M.V. De Almeida, M. Lourenço, M.V. De Souza, Synthesis and antitubercular activity of novel amino acid derivatives, Chem. Biol. Drug Des. 79 (2012) 216–222.
[35] N.C. Romeiro, G. Aguirre, P. Hernández, M. González, H. Cerecetto, I. Aldana, S. Pérez-Silanes, A. Monge, E.J. Barreiro, L.M. Lima, Synthesis, trypanocidal activity and docking studies of novel quinoxaline- *N*-acylhydrazones, designed as cruzain inhibitors candidates, Bioorg. Med. Chem. 17 (2009) 641–652.
[36] H. Cerecetto, R. Di Maio, M. González, M. Risso, P. Saenz, G. Seoane, A. Denicola, G. Peluffo, C. Quijano, C. Olea-Azar, 1, 2, 5-oxadiazole N-oxide derivatives and related compounds as potential antitrypanosomal drugs: structure-activity relationships, J. Med. Chem. 42 (1999) 1941–1950.
[37] P. Ferrara, J. Apostolakis, A. Caflisch, Evaluation of a fast implicit solvent model for molecular dynamics simulations, Proteins: Struct. Funct. Bioinf. 46 (2001) 24–33.
[38] W.C. Still, A. Tempczyk, R.C. Hawley, T. Hendrickson, Semianalytical treatment of solvation for molecular mechanics and dynamics, J. Am. Chem. Soc. 112 (1990) 6127–6129.
[39] A.K. Ghose, V.N. Viswanadhan, J.J. Wendoloski, Prediction of hydrophobic (lipophilic) properties of small organic molecules using fragmental methods: an analysis of ALOGP and CLOGP methods, J. Phys. Chem. 102 (1998) 3762–3772.
[40] V.N. Viswanadhan, A.K. Ghose, G.R. Revankar, R.K. Robins, Atomic physicochemical parameters for three dimensional structure directed quantitative structure-activity relationships. 4. Additional parameters for hydrophobic and dispersive interactions and their application for an automated superposition of certain naturally occurring nucleoside antibiotics, J. Chem. Inf. Comput. Sci. 29 (1989) 163–172.
[41] MARVINVIEW 5.4.0.1—Free License, ChemAxon Ltd., 1998–2010.
[42] H. Wiener, Structural determination of paraffin boiling points, J. Am. Chem. Soc. 69 (1947) 17–20.
[43] M. Ferreira, A.M. Antunes, M.S. Melgo, P.L.O. Volpe, Quimiometria I: calibração multivariada, um tutorial, Quim. Nova 22 (1999) 724–731.
[44] PIROUETTE 3.11, Infometrix Inc., Woodinville,WA, 1990-2003.
[45] A. Arroio, K.M. Honório, A.B.F. da Silva, Propriedades químico-quânticas empregadas em estudos das relações estrutura-atividade, Quim. Nova 33 (2010) 694–699.
[46] P.C. Mahalanobis, On the generalized distance in statistics, in: Proceedings of the National Institute of Sciences of India, New Delhi, 1936, pp. 49–55.
[47] S.D. Jorge, F. Palace-Berl, A. Masunari, C.A. Cechinel, M. Ishii, K.F.M. Pasqualoto, L.C. Tavares, Novel benzofuroxan derivatives against multidrug-resistant *Staphylococcus aureus* strains: design using Topliss' decision tree, synthesis and biological assay, Bioorg. Med. Chem. 19 (2011) 5031–5038.
[48] Origin Pro 8.0, OriginLab Corporation: 2007, One Roundhouse Plaza, Northhampton, MA, USA, 2007.
[49] B. Pniewska, M. Januchowski, Structural investigation of nifuroxazide, p-hydroxy-N′,-(5-nitrofurfurylidene) benzhydrazide, Pol. J. Chem. 72 (1998) 2629–2634.
[50] F.H. Allen, The Cambridge structural database: a quarter of a million crystal structures and rising, Acta Crystallogr. B 58 (2002) 380–388.
[51] J.L. Soares-Sobrinho, M.S. Cunha-Filho, P. Rolim Neto, J.J. Torres-Labandeira, B. Dacunha-Marinho, Benznidazole, Acta Crystallogr. Sect. E: Struct. Rep. Online E64 (2008) o634.
[52] I. Caracelli, F. Stamato, B. Mester, M. Paulino, H. Cerecetto, A new analogue of nifurtimox, Acta Crystallogr. Sect. C. Cryst. Struct. Commun. 52 (1996) 1281–1282.
[53] N.L. Allinger, Conformational analysis. 130. MM2. A hydrocarbon force field utilizing V1 and V2 torsional terms,, J. Am. Chem. Soc. 99 (1977) 8127–8134.
[54] M.J. Dewar, E.G. Zoebisch, E.F. Healy, J.J. Stewart, Development and use of quantum mechanical molecular models. 76. AM1: a new general purpose quantum mechanical molecular model, J. Am. Chem. Soc. 107 (1985) 3902–3909.
[55] D. Doherty (Ed.), MOLSIM: Molecular Mechanics and Dynamics Simulation Software-user's Guide, Version 3.2, The Chem21 Group Inc., Lake Forest, 1997.
[56] HYPERCHEM Program for Windows, Hypercube, Inc., Gainesville, FL, 2008.
[57] K. Forsythe, A. Hopfinger, The influence of solvent on the secondary structures of poly (L-alanine) and poly (L-proline),, Macromolecules 6 (1973) 423–437.
[58] G. Klopman, J.-Y. Li, S. Wang, M. Dimayuga, Computer automated log P calculations based on an extended group contribution approach, J. Chem. Inf. Comput. Sci. 34 (1994) 752–781.
[59] R. Kiralj, M. Ferreira, Is your QSAR/QSPR descriptor real or trash? J. Chemom. 24 (2010) 681–693.
[60] ViewerLite, W.L. DeLano, The Pymol Molecular Graphics System, Version1.0.DelanoScientific LLC, Palo Alto, CA, 2004. http://www.pymol.org/.
[61] C. Hansch, A. Leo, D. Hoekman, Exploring QSAR: Hydrophobic, Electronic, and Steric Constants, American Chemical Society, Washington, 1995.
[62] P.C. Mahalanobis, J. Asiat. Soc. Bengal 26 (1930) 541.